Eur. Phys. J. B (2024)97:91
https://doi.org/10.1140/epjb/s10051-024-00715-2

THE EUROPEAN PHYSICAL JOURNAL B

Regular Article - Statistical and Nonlinear Physics

# Entanglement detection in postquench nonequilibrium states: thermal Gibbs vs. generalized Gibbs ensemble

Ferenc Iglói[1,2,a] and Csaba Zoltán Király[2,b]

[1] Wigner Research Centre for Physics, Institute for Solid State Physics and Optics, Budapest 1525, Hungary
[2] Institute of Theoretical Physics, University of Szeged, Szeged 6720, Hungary

Received 29 February 2024 / Accepted 29 May 2024


**Abstract.** We use entanglement witnesses related to the entanglement negativity of the state to detect entanglement in the $XY$ chain in the postquench states in the thermodynamic limit after a quench when the parameters of the Hamiltonian are changed suddenly. The entanglement negativity is related to correlations, which in the postquench stationary state are described by a generalized Gibbs ensemble, in the ideal case. If, however, integrability breaking perturbations are present, the system is expected to thermalize. Here, we compare the nearest-neighbor entanglement in the two circumstances.

## 1 Introduction

Entanglement is a fundamental ingredient of quantum theory and has a central role in quantum information theory [1–3]. For pure states, this is directly related to correlations, while for mixed states, entanglement has a more complex meaning. A quantum state is entangled, if its density matrix cannot be written as a mixture of product states. Deciding whether a state is entangled or not is a difficult problem. However, there are conditions that are necessary and sufficient for small systems., e.g., for $2 \times 2$ (two-qubit) and $2 \times 3$ bipartite systems [4,5] and for multi-mode Gaussian states [6]. There are also conditions that are sufficient conditions for entanglement for larger systems, but does not detect all entangled states.

Considering experiments usually only limited information about the quantum state is available and this is true for theoretical calculations for very large systems. Only those approaches for entanglement detection can be applied that require the measurement of a few observables. There are entanglement conditions that are linear in operator expectation values; these are the entanglement witnesses. They are operators that have a positive expectation value for all separable states. Thus, a negative expectation value signals the presence of entanglement. The theory of entanglement witnesses has recently been rapidly developing [7–10]. It is also known how to optimize a witness operator to detect the most entangled states [9].

Apart from determining optimal entanglement witnesses, it is also important to find witnesses that are easy to measure in an experiment or possible to evaluate in a theoretical calculation. From both point of views, witnesses based on spin-chain Hamiltonians attracted considerable attention [11–17]. The energy-based witnesses have been used in various physical systems [18–23]. However, it has been shown that the optimal witness for the thermal state of the chain is not necessarily the Hamiltonian [17]. Therefore, it is recommended to consider another approach, based on a family of witnesses that detect entanglement whenever the entanglement negativity of the nearest-neighbor two-spin density matrix is nonzero [24], i.e., when the state violates the entanglement criterion based on the positivity of the partial transpose (PPT) [4,5].

For mixed states, one generally considers thermal states and calculates a temperature bound, below which the state is entangled [11–17]. Recently, however, the entanglement of other type of mixed states has also been considered, which are postquench nonequilibrium states. These states are obtained through such a protocol, when the quantum system is first placed to its ground state, and then a quench is performed, when the parameters of the Hamiltonian change suddenly [25–29]. Since the state is not an eigenstate of the new Hamiltonian, dynamics start. In the infinite time limit, the system approaches a stationary state, which is some mixture of the states appearing during the dynamics. If the Hamiltonian is nonintegrable, the system is expected to be thermalized and the stationary state is described by a Gibbs ensemble with an effective temperature [30–40]; see, however, Refs. [41–44]. For integrable systems, such as the transverse Ising chain, $XY$ and $XXY$ chains, the stationary state is assumed to be described by a so-called Generalized Gibbs Ensemble (GGE) [45–53], for which different effective temper-

[a] e-mail: igloi.ferenc@wigner.hu (corresponding author)
[b] e-mail: kiraly.csaba2000@gmail.com

Published online: 25 June 2024

atures are assigned to each conserved quantities. This type of description has been exactly calculated for the quantum Ising chain [54], and a similar formalism is conjectured for the $XY$ chain [55].

In experiments, one cannot realize such systems, which are purely integrable, since weak integrable breaking perturbations are always unavoidable. In the presence of a perturbation that breaks integrability, usual thermalization is again expected to take place. However, if the perturbation is small, the process may require a long time. On a finite time scale, the dynamics is approximately described by the evolution under the integrable unperturbed Hamiltonian. The system initially relaxes to a stationary state of the unperturbed Hamiltonian, which is called prethermalization, while genuine thermalization only occurs at later times [56–58]. This later thermalization is typically involves a thermalization time $\tau \sim \lambda^{-2}$, where $\lambda$ is the perturbation strength [59,60]. However, for specific Hamiltonians, this timescale can be much longer [61,62].

In this paper, we aim to compare the entanglement properties of a prethermalized and a genuine thermalized state. For this purpose, we use the $XY$ model, which is exactly solvable, and consider some type of integrable breaking perturbation. For the unperturbed model, several entanglement-based properties have been studied recently [63–67], and also, the postquench nonequilibrium stationary state is analyzed by energy-based and negativity-based entanglement witnesses [68]. Here, we let switch on an integrable breaking perturbation and repeat the calculation.

Our paper is organized as follows. In Sect. 2, we introduce the $XY$ model, present its free-fermion representation, calculate thermal averages, and present its conjectured GGE after a global quench. In Sect. 4, the negativity-based entanglement witness is described. In Sect. 5, the bounds for postquench states are calculated and the entangled areas are compared for prethermalized and genuine thermalized states. In Sect. 6, we close our paper with a discussion.

## 2 Model and methods

Here, we consider the $XY$ spin-chain defined by the Hamiltonian

$$\mathcal{H}_{XY} = -\sum_{l=1}^{L}\left[\frac{1+\gamma}{2}\sigma_l^x\sigma_{l+1}^x + \frac{1-\gamma}{2}\sigma_l^y\sigma_{l+1}^y\right] - h\sum_{l=1}^{L}\sigma_l^z\,, \tag{1}$$

in terms of the $\sigma_l^x$, $\sigma_l^y$, and $\sigma_l^z$ Pauli spin operators acting on the spin at site $l$, and $\sigma_{L+1}^\alpha \equiv \sigma_1^\alpha$ for $\alpha = x, y, z$. We mention that the special case $\gamma = 1$ represents the transverse Ising model, and for $h = 0$, $\gamma = 0$ the Hamiltonian reduces to the $XX$ chain.

Later, we extend the Hamiltonian with a general integrability breaking term

$$\mathcal{H} = \mathcal{H}_{XY} + \lambda\mathcal{V}(\{\boldsymbol{\sigma}\}). \tag{2}$$

This term $\mathcal{V}(\{\boldsymbol{\sigma}\})$ can c.f. contain interaction between more distant neighbors, but we do not specify its form, the rŏle of this perturbation for $\lambda \ll 1$ is to ensure thermalization of the model after a quench for sufficiently long time, $\sim \lambda^{-2}$.

### 2.1 Integrable model: $\lambda = 0$

In detail, we consider the integrable model with $\lambda = 0$, and using standard techniques [69,70], it is expressed in terms of fermion creation and annihilation operators $\eta_p^\dagger$ and $\eta_p$ as

$$\mathcal{H}_{XY} = \sum_p \varepsilon(p)\left(\eta_p^\dagger\eta_p - \frac{1}{2}\right), \tag{3}$$

where the sum runs over $L$ quasi-momenta, which are equidistant in $[-\pi, \pi]$ for periodic boundary conditions. The energy of the modes is given by [25,26,55]

$$\varepsilon(p) = 2\sqrt{\gamma^2\sin^2 p + (h-\cos p)^2} \tag{4}$$

and the Bogoliubov angle $\Theta_p$ diagonalizing the Hamiltonian is given by

$$\tan\Theta_p = -\gamma\sin p/(h-\cos p)\,. \tag{5}$$

The ground state is the fermionic vacuum, its energy being

$$E_0 = -\sum_p \frac{\varepsilon(p)}{2}. \tag{6}$$

The model has a so-called *disorder line* at

$$h_d(\gamma) = \sqrt{1-\gamma^2} \tag{7}$$

along which the ground state of the model is a product state, i.e., not entangled. For $h < h_d(\gamma)$ ($h > h_d(\gamma)$), the long-range two-point correlation functions have an (do not have) oscillatory behavior, while at $h = h_d(\gamma)$, they are constant [25,26].

At finite temperature, $T > 0$, the average value of the energy is given by

$$\langle\mathcal{H}\rangle_T = -\sum_p t(p,T)\frac{\varepsilon(p)}{2}, \tag{8}$$

with

$$t(p,T) = \tanh\left(\frac{\varepsilon(p)}{2T}\right). \tag{9}$$

(Here and in the following, we set $k_B = 1$.)

In the thermodynamic limit, $L \to \infty$, the two-point correlation functions are calculated in Refs. [25,26] and the nearest-neighbor correlations are given by

$$\begin{aligned}\langle\sigma_l^x\sigma_{l+1}^x\rangle_T &= g_c - g_s,\\ \langle\sigma_l^y\sigma_{l+1}^y\rangle_T &= g_c + g_s,\\ \langle\sigma_l^z\sigma_{l+1}^z\rangle_T &= g_0^2 - g_c^2 + g_s^2,\end{aligned} \tag{10}$$

with

$$\begin{aligned}g_c &= \frac{1}{\pi}\int_{-\pi}^{\pi} \mathrm{d}p \cos p(\cos p - h)\ t(p,T)\varepsilon^{-1}(p)\,,\\ g_s &= -\gamma\frac{1}{\pi}\int_{-\pi}^{\pi} \mathrm{d}p \sin^2 p\ t(p,T)\varepsilon^{-1}(p)\,,\\ g_0 &= \frac{1}{\pi}\int_{-\pi}^{\pi} \mathrm{d}p (h - \cos p)\ t(p,T)\varepsilon^{-1}(p)\,.\end{aligned} \tag{11}$$

## 3 Nonequilibrium stationary states after a quench

We consider global quenches at zero temperature, which suddenly change the parameters of the Hamiltonian from $\gamma_0$, $h_0$ for $t < 0$ to $\gamma$, $h$ for $t > 0$, keeping, however, the value of $\gamma_0 = \gamma$. For $t < 0$, the system is assumed to be in equilibrium, i.e., in the ground state $|\Phi_0\rangle$ of the Hamiltonian $\mathcal{H}_0$ with parameters $\gamma_0$ and $h_0$. After the quench, for $t > 0$, the state evolves coherently according to the new Hamiltonian $\mathcal{H}$ as

$$|\Phi_0(t)\rangle = \exp(-i\mathcal{H}t)\,|\Phi_0\rangle\,. \tag{12}$$

Correspondingly, the time evolution of an operator in the Heisenberg picture is

$$\sigma_l(t) = e^{i\mathcal{H}t}\sigma_l e^{-i\mathcal{H}t}. \tag{13}$$

After large enough time and in the thermodynamic limit, the system is expected to reach a stationary state

$$\boldsymbol{\rho}_q = \lim_{\tau\to\infty}\frac{1}{\tau}\int_0^{\tau} e^{-i\mathcal{H}t}|\Phi_0\rangle\langle\Phi_0|e^{+i\mathcal{H}t}\mathrm{d}t, \tag{14}$$

so that, for an observable $\mathcal{O}$, the stationary value is given by

$$\langle\mathcal{O}\rangle_{\mathrm{st}} = \mathrm{Tr}(\boldsymbol{\rho}_q\mathcal{O}). \tag{15}$$

### 3.1 Stationary values in the integrable model

In the integrable model with $\lambda = 0$, the energy of the system after the quench is given as

$$\langle\Phi_0|\mathcal{H}|\Phi_0\rangle = \sum_p \varepsilon(p)\left(\langle\Phi_0|\eta_p^\dagger\eta_p|\Phi_0\rangle - \frac{1}{2}\right), \tag{16}$$

where the occupation probability of mode $p$ in the initial state $|\Phi_0\rangle$ is given as

$$f_p = \langle\Phi_0|\,\eta_p^\dagger\eta_p\,|\Phi_0\rangle\,. \tag{17}$$

For the $XY$ model, it is expressed through the difference $\Delta_p = \Theta_p^0 - \Theta_p$ of the Bogoliubov angles as

$$f_p = \frac{1}{2}(1 - \cos\Delta_p) \tag{18}$$

with the cosine of the difference $\Delta_p$ given as

$$\cos\Delta_p = 4\frac{(\cos p - h_0)(\cos p - h) + \gamma\gamma_0\sin^2 p}{\varepsilon(p)\,\varepsilon_0(p)}, \tag{19}$$

where the index 0 refers to quantities before the quench [55]. In the thermodynamic limit, Eq. (16) can be rewritten as

$$\frac{\langle\Phi_0|\mathcal{H}|\Phi_0\rangle}{L} = -\frac{1}{4\pi}\int_{-\pi}^{\pi}\varepsilon(p)\cos\Delta_p\mathrm{d}p. \tag{20}$$

The fermions with occupation probability $f_p$ are quasiparticles, which are created homogeneously in space and the corresponding wave-packets move ballistically with constant velocity. Such a wave packet is well described by a sharp kink excitation, if the quench is performed deep into the ordered phase. Such a kink is used in the semi-classical description of the correlation functions after the quench [71]. For quenches close to the critical point, the kinks are not sharply localized and the domain walls have a finite extent of the order of the equilibrium correlation length. In this case, the semi-classical treatment should be modified. As shown in Refs. [54,55] in the thermodynamic limit, this effect can be taken into account using an effective occupation probability

$$f_p \to \tilde{f}_p = -\frac{1}{2}\ln|\cos\Delta_p|, \tag{21}$$

so that in leading order $\tilde{f}_p = f_p + \mathcal{O}(f_p^2)$.

In the stationary state, due to conserved symmetries, averages of correlations are described by a Generalized Gibbs Ensemble (GGE) [45–48,50–53]. In this case to

each fermionic mode, an effective temperature $T_{\rm eff}(p)$ is attributed through the relation [55]

$$\tanh\left(\frac{\varepsilon(p)}{2T_{\rm eff}(p)}\right) = e^{-2\tilde{f}_p} = |2f_p - 1| = |\cos\Delta_p|. \tag{22}$$

In this way, the nearest-neighbor correlations in the stationary state can be obtained as in Sect. 2.1, just replacing $t(p,T)$ defined in Eq. (9) by $|\cos\Delta_p|$

$$t(p,T) \to |\cos\Delta_p|. \tag{23}$$

In particular, we have to apply Eq. (23) for the correlation functions in Eqs. (10) and (11).

### 3.2 Stationary values in the nonintegrable model

In the nonintegrable model with $0 < \lambda \ll 1$ on finite time scale prethermalization takes place and the quasi-stationary state is described by a GGE, as explained in Sect. 3.1. After sufficiently long time, however, the system is expected to be thermalized and the genuine stationary state is expected to be described by a Gibbs ensemble. Possible ways to define a characteristic thermalization temperature, $T_{th}$, have been discussed in several papers [32,72–76]. After the quench at the prethermalization state, the different fermionic modes in the system are characterized by a set of effective temperatures in Eq. (22), and at later times in the thermalised stationary state, some average of these effective temperatures is expected. For small $\lambda$, the average value of the energy remains the same, from which the following condition for the thermalization temperature, $T_{th}$ follows:

$$\int_{-\pi}^{\pi} \varepsilon(p)\tanh\left(\frac{\varepsilon(p)}{2T_{\rm eff}(p)}\right)\mathrm{d}p = \int_{-\pi}^{\pi} \varepsilon(p)\tanh\left(\frac{\varepsilon(p)}{2T_{th}}\right)\mathrm{d}p. \tag{24}$$

Thus, the thermal stationary state is independent of the exact nature of the integrability breaking perturbations and completely characterized by the temperature $T_{th}$.

## 4 Negativity-based entanglement witness

Generally, an operator $\mathcal{W}$ is called an entanglement witness, if its expectation value, $\langle\mathcal{W}\rangle$ satisfies the following requirements [77,78]:

(i) $\langle\mathcal{W}\rangle \geq 0$ for all separable states,
(ii) $\langle\mathcal{W}\rangle < 0$ for some entangled state.

Such a state is detected by the witness as entangled. Entanglement witnesses have been used in various physical systems to verify the presence of entanglement [79–89]. We mention that a single entanglement witness cannot detect all entangled states.

Here, we consider one of the most important entanglement witness, which is connected to the partial transpose of the density matrix [4,5] and to the entanglement negativity [24]. For a bipartite density matrix given as

$$\boldsymbol{\rho} = \sum_{kl,mn} \boldsymbol{\rho}_{kl,mn}|k\rangle\langle l| \otimes |m\rangle\langle n|, \tag{25}$$

the partial transpose according to first subsystem is defined by exchanging subscripts $k$ and $l$ as

$$\boldsymbol{\rho}^{T_A} = \sum_{kl,mn} \boldsymbol{\rho}_{lk,mn}|k\rangle\langle l| \otimes |m\rangle\langle n|. \tag{26}$$

It has been shown that for separable quantum states [4,7]

$$\boldsymbol{\rho}^{T_A} \geq 0 \tag{27}$$

holds. Thus, if $\boldsymbol{\rho}^{T_A}$ has a negative eigenvalue, then the quantum state is entangled. For $2\times2$ and $2\times3$ systems, the PPT condition detects all entangled states [7]. For systems of size $3\times3$ and larger, there are PPT entangled states [5,90]. The entanglement negativity [24] is defined as

$$\mathcal{N}(\boldsymbol{\rho}) = 2\max(0, -\min(\mu_\nu)), \tag{28}$$

where $\mu_\nu$ are the eigenvalues of the partial transpose $\boldsymbol{\rho}^{T_A}$.

Let us turn to $XY$ chains and consider the nearest-neighbor reduced density matrix, $\boldsymbol{\rho}$, which is defined in the $\sigma^z$ basis. As described in details in Refs. [17,68] due to symmetries of the problem, $\boldsymbol{\rho}$ is a direct sum of two $2\times2$ matrices and the same property holds also for the partial transpose $\boldsymbol{\rho}^{T_A}$. The minimal eigenvalues of the $2\times2$ submatrices can be calculated by second-order quadrature in terms of the matrix-elements of $\boldsymbol{\rho}$. The later for the XY and Heisenberg spin chains can be expressed through nearest-neighbor correlations [64]. The final results for the minimal eigenvalues are given by [17,68]

$$\mu_{\rm min}^{(1)} = \frac{\langle\sigma_l^z\sigma_{l+1}^z\rangle + 1}{4} - \frac{1}{4}\sqrt{(\langle\sigma_l^z\rangle + \langle\sigma_{l+1}^z\rangle)^2 + (\langle\sigma_l^x\sigma_{l+1}^x\rangle + \langle\sigma_l^y\sigma_{l+1}^y\rangle)^2}\,, \tag{29}$$

and

$$\mu_{\rm min}^{(2)} = -\frac{1}{4}(\langle\sigma_l^x\sigma_{l+1}^x\rangle - \langle\sigma_l^y\sigma_{l+1}^y\rangle + \langle\sigma_l^z\sigma_{l+1}^z\rangle - 1). \tag{30}$$

The entanglement witness related to $\mu_{\min}^{(2)}$ is given by

$$\mathcal{W}_N = -\frac{1}{4}(\sigma_l^x\sigma_{l+1}^x - \sigma_l^y\sigma_{l+1}^y + \sigma_l^z\sigma_{l+1}^z - \mathbb{1}), \quad (31)$$

whereas the same for $\mu_{\min}^{(1)}$ is more complicated and derived in [68].

To proceed, we need to know that the partial transposition of a two-qubit state has at most one negative eigenvalue and all the eigenvalues lie in $[-1/2, 1]$ [91,92]. Thus, only one of the $\mu_{\min}^{(1)}$ and $\mu_{\min}^{(2)}$ can be negative, and when they are equal to each other, they must be nonnegative and the state must be separable.

## 5 Entanglement in nonequilibrium postquench states

In this section, we consider global quenches in the system, as described in Sect. 3, and study the entanglement properties of nonequilibrium stationary states, which are obtained in the large-time limit after the quench. First, we consider the prethermalized state, which is obtained by setting formally $\lambda = 0$ in Eq. (2) and having the integrable model. In this part to calculate averages, we use the GGE protocol and assign different effective temperatures to each fermionic modes, as described in Eqs. (22) and (23). Afterward, we let to switch on a small perturbation, $\lambda \ll 1$, and consider the genuine thermalized state in which there is a unique thermalization temperature as defined in Eq. (24).

We have calculated postquench states detected as entangled by the entanglement negativity-based witness using the two minimal eigenvalues, $\mu_{\min}^{(1)}$ and $\mu_{\min}^{(2)}$ in Eqs. (29) and (30), respectively. These are presented in Fig. 1 having the entangled regions where $\mu_{\min}^{(2)} < 0$, and in Fig. 2 where in the entangled regions, $\mu_{\min}^{(1)} < 0$. Entanglement detected areas in the prethermalized states are colored by violet and in the genuine thermalized states by green. Overlapping areas are colored orange. If the two parameters are equal, $h_0 = h$, which corresponds to the diagonal of the figures, the postquench state is evidently entangled. This behavior remains valid, if $h_0$ and $h$ do not differ by a large extent. If, however, they are largely different, then the postquench state becomes separable. This happens in particular if the quench is performed from the ordered state ($h_0 < 1$) to the paramagnetic state ($h > 1$).

In Fig. 1a, we consider the case with $\gamma = 1$, and hence, we have a quantum Ising chain. In this case, the negativity-based witness with $\mu_{\min}^{(2)}$ is applicable in the whole phase diagram; consequently, in Fig. 2a, there is no entangled region detected. In Fig. 1b–f, we have $\gamma < 1$, and the condition $\mu_{\min}^{(1)} < \mu_{\min}^{(2)}$ is fulfilled in a part of the phase diagram. Thus, entangled postquench states are also detected based on $\mu_{\min}^{(1)}$ and there are entangled regions in Fig. 2b–f.

Let us now consider first Fig. 1 and compare the detected entangled regions of the prethermalised and the genuine thermalised states. Here, most of the entangled regions are overlapping, but at the surfaces, there are extra regions of the genuine thermalized states. These regions are quite considerable for $\gamma$ close to 1; see the results in Fig. 1a close to $h_0 = 0$. But even in this case, there is an extra prethermalized region close to the critical point, $h_0 = 1$. We note that the detected entangled region shows non analytical behavior, both for the prethermalized and the genuine thermalized states. By reducing the value of $\gamma$, the extra thermalized region shrinks, and in the case $\gamma \ll 1$, there is even an extra entangled prethermalized region detected by the negativity-based witness with $\mu_{\min}^{(2)}$, see in Fig. 1f. If we look at Fig. 2, the trend is rather the opposite. For larger values of $\gamma$ there are extra regions belonging to the prethermalized state. These extra regions start to shrink by decreasing $\gamma$, and for very small values of $\gamma$, the thermalized states have larger entangled regions. It is interesting to compare the entangled regions in the limit $\gamma \to 0^+$. In this limit in the prethermalized state, just a part of the area is detected entangled, while in the thermalized state, the complete area is entangled. The latter behavior can be understood, while in the genuine thermalised state, the limit $\gamma \to 0^+$ is equivalent to $\gamma = 0$, when the Hamiltonians $\mathcal{H}_0$ and $\mathcal{H}$ commute and have the same ground state, which is then evidently entangled. In the prethermalised state, however different fermionic modes are occupied, than in the ground state of $\mathcal{H}_0$, which results in separable regions in Figs. 1 and 2.

## 6 Discussion

Entanglement in mixed quantum states is a difficult problem, in particular when the degrees of freedom are large and we approach the thermodynamic limit. The possible systems of investigation are usually quantum spin chains, which could have experimental realizations in condensed matter systems [93] or they could be engineered artificially through ultracold atomic gases in an optical lattice. Recently, this latter type of technique is very well developed and different intriguing questions could be studied experimentally [94–102].

In this paper, we consider the $XY$ chain, which is integrable through free-fermionic techniques and several exact results are available, mainly in the ground state, but there are some known results even at finite temperature [25,26]. We consider the entanglement properties of mixed states of the $XY$ chain, which are nonequilibrium stationary states after a quantum quench protocol. To detect entanglement, we use a family of entanglement witnesses that detect states with a nonzero bipartite entanglement negativity. In practice, this witness can detect all states that have nearest-neighbor entanglement.

The mixed states we consider are due to a quench, when parameters of the Hamiltonian of the system are

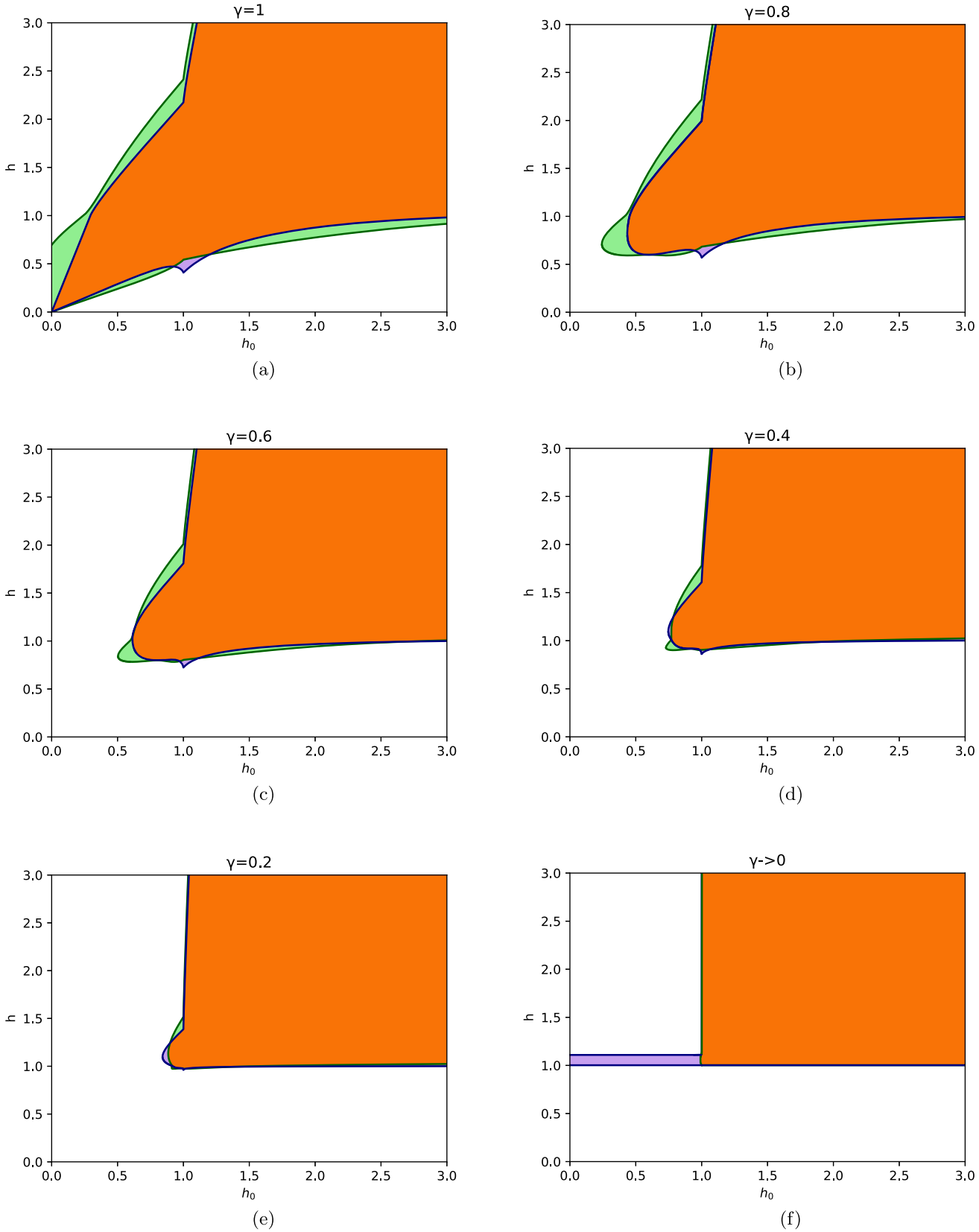


**Fig. 1** Postquench states after a sudden quench protocol $(h_0, \gamma) \to (h, \gamma)$ in the $XY$ chain. Entanglement is detected in the postquench state by the negativity-based method using $\mu^{(2)}_{\min}$ in Eq. (30): in the prethermalized state (violet) and in the genuine thermalized state (green). Overlapping areas are colored orange

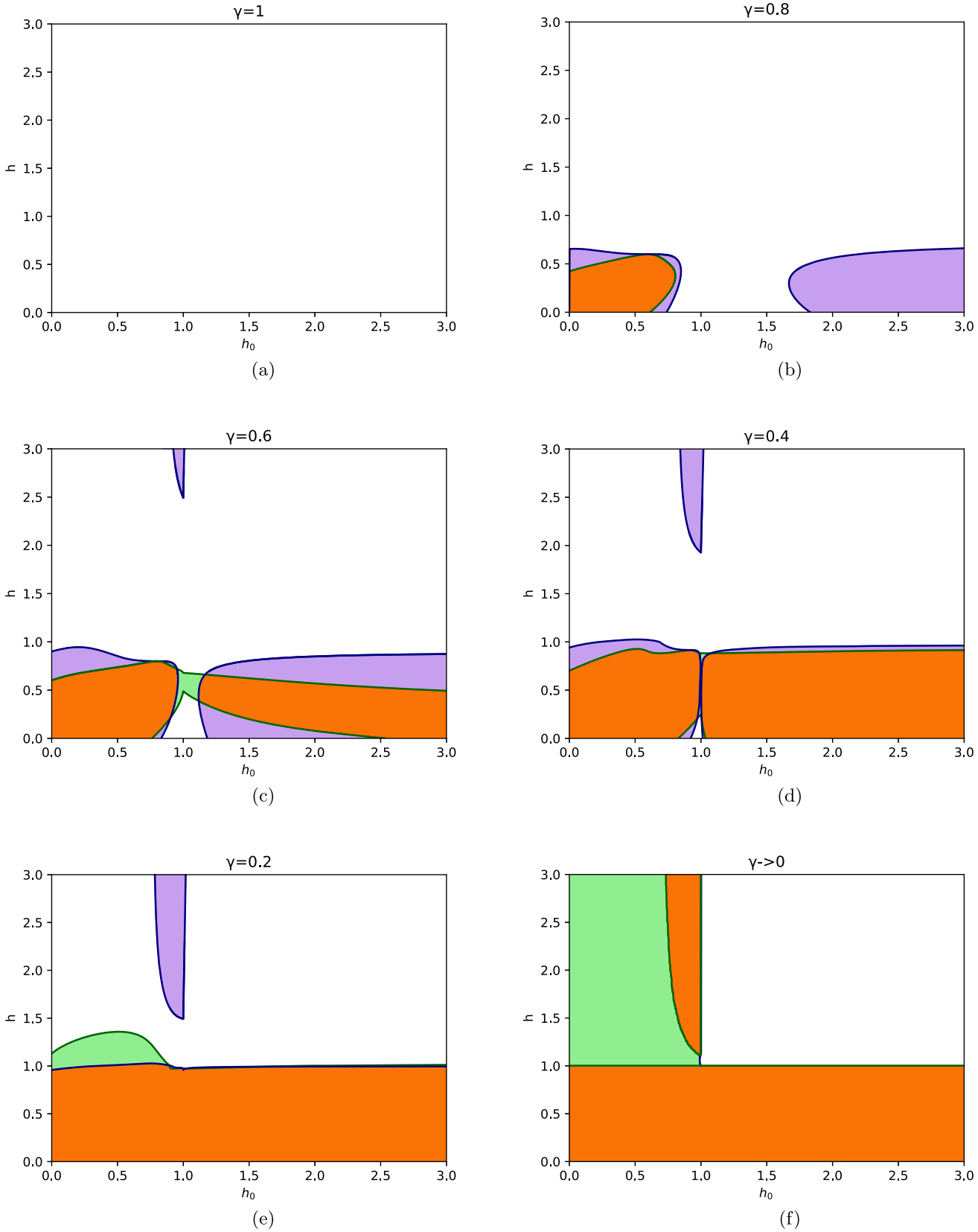


**Fig. 2** The same as in Fig. 1 but using the negativity-based method with $\mu_{\min}^{(1)}$ in Eq. (29)

changed abruptly and the time evolution of the system is governed by the new Hamiltonian. After a sufficiently long time, the system will approach a nonequilibrium stationary state, which is a mixed quantum state. For integrable systems, such as the $XY$ chain, the postquench state is described by a so-called Generalized Gibbs Ensemble, while for general, nonintegrable systems, it is expected to be a thermal state, which is described by an appropriate Gibbs ensemble. In experiments, one can not realize such systems, which are purely integrable, since weak integrable breaking perturbations are always present. If this perturbation is small, the relaxation takes part in two steps. The system initially relaxes to a stationary state of the unperturbed Hamiltonian, which is the prethermalized state, while for later times genuine thermalization takes part. In the present paper, we studied the entanglement properties of the two nonequilibrium stationary states, in particular, we want to clarify the difference between the areas detected to be entangled by the entanglement negativity witness.

The entanglement negativity in Eq. (28) for the $XY$-chain can be nonzero due to one of the two eigenvalues of the partial transpose, which are defined in Eqs.(29) and (30). Therefore, the areas which are detected entangled are indicated separately in Figs. 1 and 2 for the two cases. We observed that the areas corresponding to the prethermalized and the the genuine thermalized states are mainly overlapping; however, there are extra regions at the boundaries of the overlapping areas. For the negativity witness in Eq. (30), corresponding to Fig. 1 generally, the areas to be detected entangled increase during the thermalization process. Even in this case, there are opposite tendencies close to the critical point of the initial state. Considering the other witness in Eq. (29) and the corresponding Fig. 2 here in the prethermalized state are larger entangled areas for larger values of $\gamma$, which trend however reverse for small values of $\gamma$. We mention that it would be interesting to check the entanglement properties of postquench states of other (Bethe–Ansatz) integrable models.

While we studied the nearest-neighbor entanglement of the postquench state, other properties uncovering hidden criticality of the initial system not detectable by local quantities have recently been considered [103]. The method has been based on efficient upper bounds on the negativity in $XY$ chains [104,105]. We have shown that the criticality of the initial state can still be seen in the boundaries of the regions with nearest-neighbor entanglement.

**Acknowledgements** F.I. would like to thank G. Tóth for previous cooperation in the project and for discussions. This work was supported by the Hungarian Scientific Research Fund under Grant Nos. K128989 and No. K146736 and by the National Research, Development and Innovation Office of Hungary (NKFIH) within the Quantum Information National Laboratory of Hungary.

**Data Availability Statement** This manuscript has no associated data or the data will not be deposited. [Authors' comment: Data are available from the authors upon request].



## References

1. R. Horodecki, P. Horodecki, M. Horodecki, K. Horodecki, Quantum entanglement. Rev. Mod. Phys. **81**, 865 (2009). https://doi.org/10.1103/RevModPhys.81.865
2. O. Gühne, G. Tóth, Entanglement detection. Phys. Rep. **474**, 1 (2009). https://doi.org/10.1016/j.physrep.2009.02.004
3. N. Friis, G. Vitagliano, M. Malik, M. Huber, Entanglement certification from theory to experiment. Nat. Rev. Phys. **1**, 72 (2019). https://doi.org/10.1038/s42254-018-0003-5
4. A. Peres, Separability criterion for density matrices. Phys. Rev. Lett. **77**, 1413 (1996). https://doi.org/10.1103/PhysRevLett.77.1413
5. P. Horodecki, Separability criterion and inseparable mixed states with positive partial transposition. Phys. Lett. A **232**, 333 (1997). https://doi.org/10.1016/S0375-9601(97)00416-7
6. G. Giedke, B. Kraus, M. Lewenstein, J.I. Cirac, Entanglement criteria for all bipartite Gaussian states. Phys. Rev. Lett. **87**, 167904 (2001). https://doi.org/10.1103/PhysRevLett.87.167904
7. M. Horodecki, P. Horodecki, R. Horodecki, Separability of mixed states: necessary and sufficient conditions. Phys. Lett. A **223**, 1 (1996). https://doi.org/10.1016/S0375-9601(96)00706-2
8. B.M. Terhal, Bell inequalities and the separability criterion. Phys. Lett. A **271**, 319 (2000). https://doi.org/10.1016/S0375-9601(00)00401-1
9. M. Lewenstein, B. Kraus, J.I. Cirac, P. Horodecki, Optimization of entanglement witnesses. Phys. Rev. A **62**, 052310 (2000). https://doi.org/10.1103/PhysRevA.62.052310
10. A. Acín, D. Bruß, M. Lewenstein, A. Sanpera, Classification of mixed three-qubit states. Phys. Rev. Lett. **87**, 040401 (2001). https://doi.org/10.1103/PhysRevLett.87.040401

11. G. Tóth, Entanglement witnesses in spin models. Phys. Rev. A **71**, 010301(R) (2005). https://doi.org/10.1103/PhysRevA.71.010301
12. G. Tóth, O. Gühne, Detection of multipartite entanglement with two-body correlations. Appl. Phys. B **82**, 237 (2006). https://doi.org/10.1007/s00340-005-2057-1
13. O. Gühne, G. Tóth, Energy and multipartite entanglement in multidimensional and frustrated spin models. Phys. Rev. A **73**, 052319 (2006). https://doi.org/10.1103/PhysRevA.73.052319
14. O. Gühne, G. Tóth, H.J. Briegel, Multipartite entanglement in spin chains. New J. Phys **7**, 229 (2005)
15. C. Brukner, V. Vedral, Macroscopic Thermodynamical Witnesses of Quantum Entanglement (2004). arXiv:quant-ph/0406040
16. M.R. Dowling, A.C. Doherty, S.D. Bartlett, Energy as an entanglement witness for quantum many-body systems. Phys. Rev. A **70**, 062113 (2004). https://doi.org/10.1103/PhysRevA.70.062113
17. L.-A. Wu, S. Bandyopadhyay, M.S. Sarandy, D.A. Lidar, Entanglement observables and witnesses for interacting quantum spin systems. Phys. Rev. A **72**, 032309 (2005). https://doi.org/10.1103/PhysRevA.72.032309
18. T. Vértesi, E. Bene, Thermal entanglement in the nanotubular system $Na_2V_3O_7$. Phys. Rev. B **73**, 134404 (2006). https://doi.org/10.1103/PhysRevB.73.134404
19. I. Siloi, F. Troiani, Towards the chemical tuning of entanglement in molecular nanomagnets. Phys. Rev. B **86**, 224404 (2012). https://doi.org/10.1103/PhysRevB.86.224404
20. I. Siloi, F. Troiani, Quantum entanglement in heterometallic wheels. Eur. Phys. J. B **86**, 71 (2013). https://doi.org/10.1140/epjb/e2012-30681-1
21. F. Troiani, I. Siloi, Energy as a witness of multipartite entanglement in chains of arbitrary spins. Phys. Rev. A **86**, 032330 (2012). https://doi.org/10.1103/PhysRevA.86.032330
22. T. Homayoun, K. Aghayar, Energy as an entanglement witnesses for one dimensional XYZ Heisenberg lattice: optimization approach. J. Stat. Phys. **176**, 85 (2019). https://doi.org/10.1007/s10955-019-02289-1
23. F. Troiani, S. Carretta, P. Santini, Detection of entanglement between collective spins. Phys. Rev. B **88**, 195421 (2013). https://doi.org/10.1103/PhysRevB.88.195421
24. G. Vidal, R.F. Werner, Computable measure of entanglement. Phys. Rev. A **65**, 032314 (2002). https://doi.org/10.1103/PhysRevA.65.032314
25. E. Barouch, B.M. McCoy, M. Dresden, Statistical mechanics of the XY model. I. Phys. Rev. A **2**, 1075 (1970). https://doi.org/10.1103/PhysRevA.2.1075
26. E. Barouch, B.M. McCoy, Statistical mechanics of the XY model. III. Phys. Rev. A **3**, 2137 (1971). https://doi.org/10.1103/PhysRevA.3.2137
27. F. Iglói, H. Rieger, Long-range correlations in the nonequilibrium quantum relaxation of a spin chain. Phys. Rev. Lett. **85**, 3233 (2000). https://doi.org/10.1103/PhysRevLett.85.3233
28. K. Sengupta, S. Powell, S. Sachdev, Quench dynamics across quantum critical points. Phys. Rev. A **69**, 053616 (2004). https://doi.org/10.1103/PhysRevA.69.053616
29. A. Polkovnikov, K. Sengupta, A. Silva, M. Vengalattore, Colloquium: nonequilibrium dynamics of closed interacting quantum systems. Rev. Mod. Phys. **83**, 863 (2011). https://doi.org/10.1103/RevModPhys.83.863
30. S. Sotiriadis, D. Fioretto, G. Mussardo, Zamolodchikov–Faddeev algebra and quantum quenches in integrable field theories. J. Stat. Mech. Theory Exp. **02**, P02017 (2012). https://doi.org/10.1088/1742-5468/2012/02/p02017
31. G. Roux, Quenches in quantum many-body systems: one-dimensional Bose–Hubbard model reexamined. Phys. Rev. A **79**, 021608 (2009). https://doi.org/10.1103/PhysRevA.79.021608
32. S. Sotiriadis, P. Calabrese, J. Cardy, Quantum quench from a thermal initial state. Europhys. Lett. **87**, 20002 (2009). https://doi.org/10.1209/0295-5075/87/20002
33. M. Kollar, M. Eckstein, Relaxation of a one-dimensional Mott insulator after an interaction quench. Phys. Rev. A **78**, 013626 (2008). https://doi.org/10.1103/PhysRevA.78.013626
34. T. Barthel, U. Schollwöck, Dephasing and the steady state in quantum many-particle systems. Phys. Rev. Lett. **100**, 100601 (2008). https://doi.org/10.1103/PhysRevLett.100.100601
35. M. Cramer, A. Flesch, I.P. McCulloch, U. Schollwöck, J. Eisert, Exploring local quantum many-body relaxation by atoms in optical superlattices. Phys. Rev. Lett. **101**, 063001 (2008). https://doi.org/10.1103/PhysRevLett.101.063001
36. M. Cramer, C.M. Dawson, J. Eisert, T.J. Osborne, Exact relaxation in a class of nonequilibrium quantum lattice systems. Phys. Rev. Lett. **100**, 030602 (2008). https://doi.org/10.1103/PhysRevLett.100.030602
37. S.R. Manmana, S. Wessel, R.M. Noack, A. Muramatsu, Strongly correlated fermions after a quantum quench. Phys. Rev. Lett. **98**, 210405 (2007). https://doi.org/10.1103/PhysRevLett.98.210405
38. M.A. Cazalilla, Effect of suddenly turning on interactions in the Luttinger model. Phys. Rev. Lett. **97**, 156403 (2006). https://doi.org/10.1103/PhysRevLett.97.156403
39. P. Calabrese, J. Cardy, Time dependence of correlation functions following a quantum quench. Phys. Rev. Lett. **96**, 136801 (2006). https://doi.org/10.1103/PhysRevLett.96.136801
40. M. Rigol, V. Dunjko, V. Yurovsky, M. Olshanii, Relaxation in a completely integrable many-body quantum system: an ab initio study of the dynamics of the highly excited states of 1D lattice hard-core bosons. Phys. Rev. Lett. **98**, 050405 (2007). https://doi.org/10.1103/PhysRevLett.98.050405
41. R. Hamazaki, T.N. Ikeda, M. Ueda, Generalized Gibbs ensemble in a nonintegrable system with an extensive number of local symmetries. Phys. Rev. E **93**, 032116 (2016). https://doi.org/10.1103/PhysRevE.93.032116
42. J. Larson, Integrability versus quantum thermalization. J. Phys. B Atom. Mol. Opt. Phys. **46**, 224016 (2013). https://doi.org/10.1088/0953-4075/46/22/224016
43. V.A. Yurovsky, M. Olshanii, Memory of the initial conditions in an incompletely chaotic quantum system:

universal predictions with application to cold atoms. Phys. Rev. Lett. **106**, 025303 (2011). https://doi.org/10.1103/PhysRevLett.106.025303
44. M. Olshanii, K. Jacobs, M. Rigol, V. Dunjko, H. Kennard, V.A. Yurovsky, An exactly solvable model for the integrability-chaos transition in rough quantum billiards. Nat. Commun. **3**, 641 (2012). https://doi.org/10.1038/ncomms1653
45. L. Vidmar, M. Rigol, Generalized Gibbs ensemble in integrable lattice models. J. Stat. Mech. Theory Exp. **2016**(6), 064007 (2016). https://doi.org/10.1088/1742-5468/2016/06/064007
46. E. Ilievski, M. Medenjak, T. Prosen, L. Zadnik, Quasilocal charges in integrable lattice systems. J. Stat. Mech. Theory Exp. **2016**(6), 064008 (2016). https://doi.org/10.1088/1742-5468/2016/06/064008
47. E. Ilievski, J. De Nardis, B. Wouters, J.-S. Caux, F.H.L. Essler, T. Prosen, Complete generalized Gibbs ensembles in an interacting theory. Phys. Rev. Lett. **115**, 157201 (2015). https://doi.org/10.1103/PhysRevLett.115.157201
48. F.H.L. Essler, G. Mussardo, M. Panfil, Generalized Gibbs ensembles for quantum field theories. Phys. Rev. A **91**, 051602 (2015). https://doi.org/10.1103/PhysRevA.91.051602
49. B. Pozsgay, Quantum quenches and generalized Gibbs ensemble in a Bethe Ansatz solvable lattice model of interacting bosons. J. Stat. Mech. Theory Exp. **2014**(10), P10045 (2014). https://doi.org/10.1088/1742-5468/2014/10/p10045
50. B. Pozsgay, Failure of the generalized eigenstate thermalization hypothesis in integrable models with multiple particle species. J. Stat. Mech. Theory Exp. **2014**(9), P09026 (2014). https://doi.org/10.1088/1742-5468/2014/09/p09026
51. G. Goldstein, N. Andrei, Failure of the local generalized Gibbs ensemble for integrable models with bound states. Phys. Rev. A **90**, 043625 (2014). https://doi.org/10.1103/PhysRevA.90.043625
52. B. Pozsgay, M. Mestyán, M.A. Werner, M. Kormos, G. Zaránd, G. Takács, Correlations after quantum quenches in the $XXZ$ spin chain: failure of the generalized Gibbs ensemble. Phys. Rev. Lett. **113**, 117203 (2014). https://doi.org/10.1103/PhysRevLett.113.117203
53. B. Wouters, J. De Nardis, M. Brockmann, D. Fioretto, M. Rigol, J.-S. Caux, Quenching the anisotropic heisenberg chain: exact solution and generalized Gibbs ensemble predictions. Phys. Rev. Lett. **113**, 117202 (2014). https://doi.org/10.1103/PhysRevLett.113.117202
54. P. Calabrese, F.H.L. Essler, M. Fagotti, Quantum quench in the transverse field ising chain: I. time evolution of order parameter correlators. J. Stat. Mech. Theory Exp. **2012**(07), P07016 (2012). https://doi.org/10.1088/1742-5468/2012/07/p07016
55. B. Blass, H. Rieger, F. Iglói, Quantum relaxation and finite-size effects in the XY chain in a transverse field after global quenches. EPL (Europhys. Lett.) **99**, 30004 (2012). https://doi.org/10.1209/0295-5075/99/30004
56. J. Berges, S. Borsányi, C. Wetterich, Prethermalization. Phys. Rev. Lett. **93**, 142002 (2004). https://doi.org/10.1103/PhysRevLett.93.142002
57. M. Kollar, F.A. Wolf, M. Eckstein, Generalized Gibbs ensemble prediction of prethermalization plateaus and their relation to nonthermal steady states in integrable systems. Phys. Rev. B **84**, 054304 (2011). https://doi.org/10.1103/PhysRevB.84.054304
58. T. Langen, T. Gasenzer, J. Schmiedmayer, Prethermalization and universal dynamics in near-integrable quantum systems. J. Stat. Mech. Theory Exp. **2016**, 064009 (2016). https://doi.org/10.1088/1742-5468/2016/06/064009
59. K. Mallayya, M. Rigol, W. De Roeck, Prethermalization and thermalization in isolated quantum systems. Phys. Rev. X **9**, 021027 (2019). https://doi.org/10.1103/PhysRevX.9.021027
60. K. Mallayya, M. Rigol, Prethermalization, thermalization, and Fermi's golden rule in quantum many-body systems. Phys. Rev. B **104**, 184302 (2021). https://doi.org/10.1103/PhysRevB.104.184302
61. D. Abanin, W. De Roeck, W.W. Ho, F. Huveneers, A rigorous theory of many-body prethermalization for periodically driven and closed quantum systems. Commun. Math. Phys. **354**, 809 (2017). https://doi.org/10.1007/s00220-017-2930-x
62. F.M. Surace, O. Motrunich, Weak integrability breaking perturbations of integrable models (2023). arXiv:2302.12804 [cond-mat.stat-mech]
63. A. Osterloh, L. Amico, G. Falci, R. Fazio, Scaling of entanglement close to a quantum phase transition. Nature (Lond.) **416**, 608 (2002). https://doi.org/10.1038/416608a
64. T.J. Osborne, M.A. Nielsen, Entanglement in a simple quantum phase transition. Phys. Rev. A **66**, 032110 (2002). https://doi.org/10.1103/PhysRevA.66.032110
65. D. Patanè, R. Fazio, L. Amico, Bound entanglement in the XY model. New J. Phys. **9**, 322 (2007). https://doi.org/10.1088/1367-2630/9/9/322
66. M. Hofmann, A. Osterloh, O. Gühne, Scaling of genuine multiparticle entanglement close to a quantum phase transition. Phys. Rev. B **89**, 134101 (2014). https://doi.org/10.1103/PhysRevB.89.134101
67. S.M. Giampaolo, B.C. Hiesmayr, Genuine multipartite entanglement in the $xy$ model. Phys. Rev. A **88**, 052305 (2013). https://doi.org/10.1103/PhysRevA.88.052305
68. F. Iglói, G. Tóth, Entanglement witnesses in the $xy$ chain: thermal equilibrium and postquench nonequilibrium states. Phys. Rev. Res. **5**, 013158 (2023). https://doi.org/10.1103/PhysRevResearch.5.013158
69. E. Lieb, T. Schultz, D. Mattis, Two soluble models of an antiferromagnetic chain. Ann. Phys. **16**, 407 (1961). https://doi.org/10.1016/0003-4916(61)90115-4
70. P. Pfeuty, The one-dimensional Ising model with a transverse field. Ann. Phys. **57**, 79 (1970). https://doi.org/10.1016/0003-4916(70)90270-8
71. H. Rieger, F. Iglói, Semiclassical theory for quantum quenches in finite transverse ising chains. Phys. Rev. B **84**, 165117 (2011). https://doi.org/10.1103/PhysRevB.84.165117
72. D. Rossini, A. Silva, G. Mussardo, G.E. Santoro, Effective thermal dynamics following a quantum quench in a spin chain. Phys. Rev. Lett. **102**, 127204 (2009). https://doi.org/10.1103/PhysRevLett.102.127204
73. D. Rossini, S. Suzuki, G. Mussardo, G.E. Santoro, A. Silva, Long time dynamics following a quench in

an integrable quantum spin chain: local versus non-local operators and effective thermal behavior. Phys. Rev. B **82**, 144302 (2010). https://doi.org/10.1103/PhysRevB.82.144302
74. M. Rigol, Quantum quenches and thermalization in one-dimensional fermionic systems. Phys. Rev. A **80**, 053607 (2009). https://doi.org/10.1103/PhysRevA.80.053607
75. E. Canovi, D. Rossini, R. Fazio, G.E. Santoro, A. Silva, Quantum quenches, thermalization, and many-body localization. Phys. Rev. B **83**, 094431 (2011). https://doi.org/10.1103/PhysRevB.83.094431
76. L. Foini, L.F. Cugliandolo, A. Gambassi, Fluctuation–dissipation relations and critical quenches in the transverse field ising chain. Phys. Rev. B **84**, 212404 (2011). https://doi.org/10.1103/PhysRevB.84.212404
77. M. Lewenstein, B. Kraus, P. Horodecki, J.I. Cirac, Characterization of separable states and entanglement witnesses. Phys. Rev. A **63**, 044304 (2001). https://doi.org/10.1103/PhysRevA.63.044304
78. B.M. Terhal, Detecting quantum entanglement. Theor. Comput. Sci. **287**, 313 (2002). https://doi.org/10.1016/S0304-3975(02)00139-1
79. M. Bourennane, M. Eibl, C. Kurtsiefer, S. Gaertner, H. Weinfurter, O. Gühne, P. Hyllus, D. Bruß, M. Lewenstein, A. Sanpera, Experimental detection of multipartite entanglement using witness operators. Phys. Rev. Lett. **92**, 087902 (2004). https://doi.org/10.1103/PhysRevLett.92.087902
80. P. Walther, K.J. Resch, T. Rudolph, E. Schenck, H. Weinfurter, V. Vedral, M. Aspelmeyer, A. Zeilinger, Experimental one-way quantum computing. Nature (Lond.) **434**, 169 (2005). https://doi.org/10.1038/nature03347
81. N. Kiesel, C. Schmid, U. Weber, G. Tóth, O. Gühne, R. Ursin, H. Weinfurter, Experimental analysis of a four-qubit photon cluster state. Phys. Rev. Lett. **95**, 210502 (2005). https://doi.org/10.1103/PhysRevLett.95.210502
82. W. Wieczorek, R. Krischek, N. Kiesel, P. Michelberger, G. Tóth, H. Weinfurter, Experimental entanglement of a six-photon symmetric dicke state. Phys. Rev. Lett. **103**, 020504 (2009). https://doi.org/10.1103/PhysRevLett.103.020504
83. R. Prevedel, G. Cronenberg, M.S. Tame, M. Paternostro, P. Walther, M.S. Kim, A. Zeilinger, Experimental realization of dicke states of up to six qubits for multiparty quantum networking. Phys. Rev. Lett. **103**, 020503 (2009). https://doi.org/10.1103/PhysRevLett.103.020503
84. W.-B. Gao, C.-Y. Lu, X.-C. Yao, P. Xu, O. Gühne, A. Goebel, Y.-A. Chen, C.-Z. Peng, Z.-B. Chen, J.-W. Pan, Experimental demonstration of a hyper-entangled ten-qubit schrödinger cat state. Nat. Phys. **6**, 331 (2010). https://doi.org/10.1038/nphys1603
85. M. Gong, M.-C. Chen, Y. Zheng, S. Wang, C. Zha, H. Deng, Z. Yan, H. Rong, Y. Wu, S. Li, F. Chen, Y. Zhao, F. Liang, J. Lin, Y. Xu, C. Guo, L. Sun, A.D. Castellano, H. Wang, C. Peng, C.-Y. Lu, X. Zhu, J.-W. Pan, Genuine 12-qubit entanglement on a superconducting quantum processor. Phys. Rev. Lett. **122**, 110501 (2019). https://doi.org/10.1103/PhysRevLett.122.110501
86. H. Häffner, W. Hänsel, C. Roos, J. Benhelm, M. Chwalla, T. Körber, U. Rapol, M. Riebe, P. Schmidt, C. Becher, O. Gühne, W. Dür, R. Blatt, Scalable multiparticle entanglement of trapped ions. Nature (Lond.) **438**, 643 (2005). https://doi.org/10.1038/nature04279
87. T. Monz, P. Schindler, J.T. Barreiro, M. Chwalla, D. Nigg, W.A. Coish, M. Harlander, W. Hänsel, M. Hennrich, R. Blatt, 14-Qubit entanglement: creation and coherence. Phys. Rev. Lett. **106**, 130506 (2011). https://doi.org/10.1103/PhysRevLett.106.130506
88. E.B. Fel'dman, A.N. Pyrkov, Evolution of spin entanglement and an entanglement witness in multiple-quantum nmr experiments. JETP Lett. **88**, 398 (2008). https://doi.org/10.1134/S0021364008180124
89. M. Gärttner, P. Hauke, A.M. Rey, Relating out-of-time-order correlations to entanglement via multiple-quantum coherences. Phys. Rev. Lett. **120**, 040402 (2018). https://doi.org/10.1103/PhysRevLett.120.040402
90. M. Horodecki, P. Horodecki, R. Horodecki, Mixed-state entanglement and distillation: is there a "bound" entanglement in nature? Phys. Rev. Lett. **80**, 5239 (1998). https://doi.org/10.1103/PhysRevLett.80.5239
91. A. Sanpera, R. Tarrach, G. Vidal, Local description of quantum inseparability. Phys. Rev. A **58**, 826 (1998). https://doi.org/10.1103/PhysRevA.58.826
92. S. Rana, Negative eigenvalues of partial transposition of arbitrary bipartite states. Phys. Rev. A **87**, 054301 (2013). https://doi.org/10.1103/PhysRevA.87.054301
93. A. Dutta, G. Aeppli, B.K. Chakrabarti, U. Divakaran, T.F. Rosenbaum, D. Sen, *Quantum Phase Transitions in Transverse Field Spin Models: From Statistical Physics to Quantum Information* (Cambridge University Press, Cambridge, 2015)
94. M. Greiner, O. Mandel, T.W. Hänsch, I. Bloch, Collapse and revival of the matter wave field of a Bose–Einstein condensate. Nature (Lond.) **419**, 51 (2002). https://doi.org/10.1038/nature00968
95. B. Paredes, A. Widera, V. Murg, O. Mandel, S. Fölling, I. Cirac, G.V. Shlyapnikov, T.W. Hänsch, I. Bloch, Tonks–Girardeau gas of ultracold atoms in an optical lattice. Nature (Lond.) **429**, 277 (2004). https://doi.org/10.1038/nature02530
96. L.E. Sadler, J.M. Higbie, S.R. Leslie, M. Vengalattore, D.M. Stamper-Kurn, Spontaneous symmetry breaking in a quenched ferromagnetic spinor Bose–Einstein condensate. Nature (Lond.) **443**, 312 (2006). https://doi.org/10.1038/nature05094
97. A. Lamacraft, Quantum quenches in a spinor condensate. Phys. Rev. Lett. **98**, 160404 (2007). https://doi.org/10.1103/PhysRevLett.98.160404
98. T. Kinoshita, T. Wenger, D.S. Weiss, A quantum newton's cradle. Nature (Lond.) **440**, 900 (2006). https://doi.org/10.1038/nature04693
99. S. Hofferberth, I. Lesanovsky, B. Fischer, T. Schumm, J. Schmiedmayer, Non-equilibrium coherence dynamics in one-dimensional Bose gases. Nature (Lond.) **449**, 324 (2007). https://doi.org/10.1038/nature06149
100. I. Bloch, J. Dalibard, W. Zwerger, Many-body physics with ultracold gases. Rev. Mod. Phys. **80**, 885 (2008). https://doi.org/10.1103/RevModPhys.80.885
101. S. Trotzky, Y.-A. Chen, A. Flesch, I.P. McCulloch, U. Schollwöck, J. Eisert, I. Bloch, Probing the relaxation

towards equilibrium in an isolated strongly correlated one-dimensional Bose gas. Nat. Phys. **8**, 325 (2012). https://doi.org/10.1038/nphys2232

102. M. Cheneau, P. Barmettler, D. Poletti, M. Endres, P. Schauß, T. Fukuhara, C. Gross, I. Bloch, C. Kollath, S. Kuhr, Light-cone-like spreading of correlations in a quantum many-body system. Nature (Lond.) **481**, 484 (2012). https://doi.org/10.1038/nature10748
103. S. Paul, P. Titum, M.F. Maghrebi, Hidden quantum criticality and entanglement in quench dynamics. arXiv:2202.04654 (2022)
104. V. Eisler, Z. Zimborás, On the partial transpose of fermionic gaussian states. New J. Phys. **17**, 053048 (2015). https://doi.org/10.1088/1367-2630/17/5/053048
105. J. Eisert, V. Eisler, Z. Zimborás, Entanglement negativity bounds for fermionic gaussian states. Phys. Rev. B **97**, 165123 (2018). https://doi.org/10.1103/PhysRevB.97.165123